

Infrared Spectra of Aluminum Fluorocarbon Polymer Compositions to Thermal Signature of Jet Engine

Amir Elsaïdy*, Mohamed Kassem, Hesham Tantawy, Sherif Elbasuney and Gaber Zaky M

School of Chemical Engineering, Military Technical College, Kobry Elkoba, Cairo, Egypt

Research Article

Received: 17/09/2018

Accepted: 09/10/2018

Published: 16/10/2018

*For Correspondence

Amir Elsaïdy, School of Chemical Engineering,
Military Technical College, Egypt.

Tel: 61 2 9385 8100

E-mail: amir.alsaïdy@mtc.edu.eg

Keywords: Decoy flares, ATV, Infrared,
Spectroscopy, Thermal signature.

ABSTRACT

Flares are energetic materials, which can yield thermal signature that can interfere with infrared guided missiles. Flare thermal signature should be similar to aircraft but with higher intensity; this signature depends on exothermal reaction as well as the chemical nature of combustion products. Aluminum is the most common reactive metal fuel in use in energetic systems as it can offer high heat output (32000 J/g) as well as superior chemical stability. In this study, different flare formulations based on aluminum as a fuel, fluorocarbon polymer (Teflon) as an oxidizer, and Viton as a binder (with fuel percentage from 40:70 wt%) were developed by granulation and subsequent pressing. The spectral performance of developed formulations was evaluated to the thermal signature of aircraft jet engine using (FT-MIR 2-6 μm) spectrophotometer. The thermal signature of jet engine was characterized with two characteristic peaks over α (2-3 μm) and β (3-5 μm) band; this signature was correlated to black body emission by the hot nozzle at 690°C. The developed flares offered similar thermal signature but with higher intensity. Aluminum/Teflon/Viton (ATV) flare, with 50 wt% Al, offered an increase in the intensity of α band and β by 6 and 1.5 times respectively. The developed ATV flare offered characteristic intensity ratio Θ (I_{α}/I_{β}) (the main spectral parameter) of 0.73; this value was found to be in good accordance with literature. Quantification of infrared emitting species as well as combustion temperature was conducted using the ICT thermodynamic code. ATV flare (50 wt% Al) offered the highest percentage (78.1 wt%) of AlF the main IR emitting species as well as 12.1 wt% of C soot which is an ideal black body emitter. This is manuscript would open the route for the development of flares with tailored spectral performance.

INTRODUCTION

Infrared (IR) guided missiles represent the major threat to military aircrafts; they resulted in 90% of aircraft damage^[1]. IR seekers can detect IR radiation; subsequently it can identify the aircraft as a potential target^[2,3]. Aircraft thermal signature is generated via several components including: the metal skin, jet engine, and exhaust. The aircraft fuselage emits between 8-10 μm , due to sun radiation or air friction. Emission over the range of 3-5 μm is resulted from hot exhaust gases (H_2O , CO , CO_2). Hot jet engine emits in the range of 2-2.5 μm (**Figure 1**)^[2].

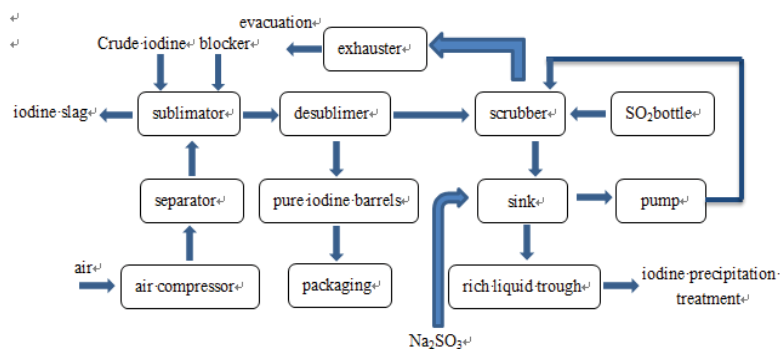


Figure 1: Main infrared radiation sources of an aircraft.

Heat-seeking missiles search for radiation released from the aircraft over α (2-3 μm) and β (4-5 μm) bands with relative intensity ration [4]. Decoy flare is the main countermeasure technique that can be employed to protect aircraft against thermal detectors [5].

Standard flares consist mainly of Magnesium (fuel), Teflon (oxidizer), and Viton (binder); they are commonly known as MTV flares [2,6]. Nowadays, aluminum is the fuel of interest for different pyrotechnic formulations due to its high heat output (32000 J/g) and high chemical stability [7-10]. While aluminum metal fuel can develop a protective oxide layer offering extended storage time without loss of reactivity (Figure 2); magnesium fuel suffers from lack of chemical stability. Mg is susceptible to acid and humidity with the formation of $\text{Mg}(\text{OH})_2$ with loss of reactivity [11].

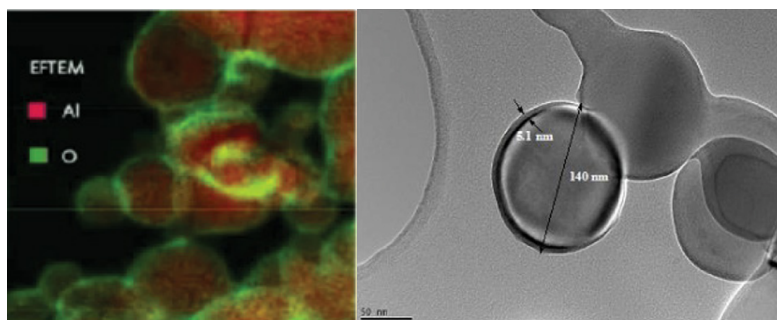


Figure 2: Aluminium particles with protective oxide layer of Al_2O_3 .

Aluminum can act as high energy density material; it has found wide applications in different energetic systems [12]. Straight way to increase the overall released energy, can be achieved by incorporating reactive metal fuel (i. e. Al) into the energetic system [13-15]. Aluminum can react not only with free oxidizing element (oxygen/fluorine) available from oxidizer; but also it can react inert gasses adding substantial heat output [16].



These set of reactions can offer substantial heat ouptput. Furthermore, Al can find wide application in thermite reactions. Thermite particles composed of $\text{Al}/\text{Fe}_2\text{O}_3$, $\text{Sr}(\text{NO}_3)_2$, were combined with energetic binder to develop the so-called “pyro-organic” flare formulations; this flare demonstrated a promising relative intensity ratio(θ) under dynamic conditions [17].

The relative intensity ratio (θ) is defined as the ratio of the average intensity in the α band (2-3 μm) to the average intensity of the β band (3-5 μm) (Eqn. (6)).

$$\theta = I_\alpha / I_\beta \tag{6}$$

For IR emitting flares, it is important to offer not only thermal signature similar to aircraft but also the relative intensity ratio should be comparable to aircraft. Consequently the main parameters for effective development of decoy flare include:

- High emissivity values.
- High combustion temperatures.
- θ value lies between 0.5-0.8.

For an aircraft, θ value in the range of 0.7; recent decoy flares offered θ values of 1.3-1.4 [2,4]. This study is dedicated to the effective development of novel decoy flare that can offer high emissivity, high combustion temperature, and with Θ value similar to that of the aircraft. Flare with such characteristics could be an effective countermeasure against infrared missiles attacks. The development of decoy flare with controlled radiant intensity requires physical and chemical means to be applied [1,18-28].

Research studies conducted on Aluminum/Teflon/Viton mixtures were limited to burning temperature and burning rate no information about thermal signature has been reported [29,30]. In this study, thermal signature of jet engine (jet cat p200 sx) was measured using (FT-MIR 1-6 μm) spectrophotometer. The characteristic intensity ratio for this engine was calculated. ATV flares with different fuel percentage were prepared and pressed in the desired dimensions. The spectral performance of developed flares was measured and compared to jet engine thermal signature. Quantification of combustion temperature and the main active emitting species (c soot (nearly ideal emitter), AlF (molecular emitter), and Al (heat source)) in the combustion flame was conducted using ICT Thermodynamic Code (Institute of Chemical Technology in Germany, virgin 2008). ATV flare with 50 wt% Al offered higher intensity over α band (2-3 μm) and β band α band (2-3 μm) by 6 and 1.5 times respectively. The main outcome of this study is that this novel flare offered Θ value of 0.73.

EXPERIMENTAL WORK

Thermal Signature of Jet Engine Nozzle

Thermal signature of jet engine nozzle (jet cat P200 SX turbine with heavy-duty starter) was measured using (FT-MIR 2-6) spectrophotometer (Figure 3).

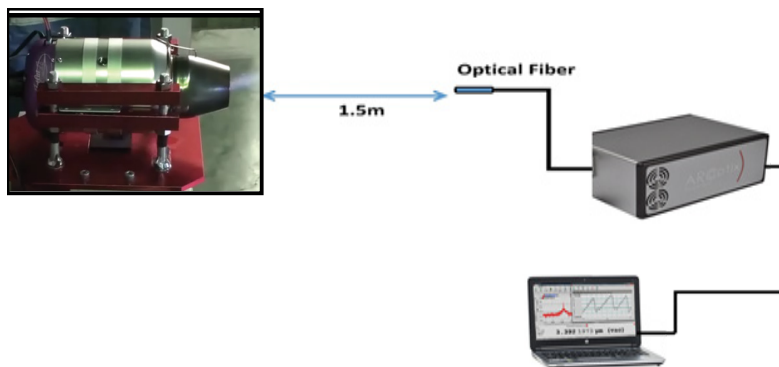


Figure 3: Schematic for thermal signature measurements of jet engine nozzle.

Decoy Flare Formulation

Chemicals and materials: The main constituents for flares manufacture include oxidizer, metal fuel, and binder. Teflon can act as an oxidizer; Viton A can act as plasticizer and binder. Table 1 tabulates a list of chemicals used in this study.

Table 1: The function and structure of different used chemicals.

Chemicals	Function	Function	Grade	Supplier
Teflon	oxidizer	$[-CF_2 - CF_2 -]_n$	n= 20000 fine powder	Alpha
Aluminum	fuel	Al	fine powder	Alpha
Viton A	binder	$[-CH_2 - CF_2 - CF_2 - CF_3 -]_m$	1.85 g/cm ³ fluorine: 65%	Alpha

An efficient study, to develop ATV flares with improved spectral performance was performed. This study includes the following main steps:

- Fuel percentage range (40:70) wt%
- Oxidizer percentage range (25:55) wt%
- Binder percentage 5 wt%

Table 2 summarizes the chemical composition of different investigated ATV formulations.

Table 2: Chemical composition of developed decoy flares.

Formulation	Al	Teflon	Viton A
	wt%	wt%	wt%
F ₁	40	55	5
F ₂	45	50	5
F ₃	50	45	5
F ₄	55	40	5
F ₅	60	35	5
F ₆	65	30	5
F ₇	70	25	5

Development technology of decoy flares, should emphasize mixing and homogeneity of different ingredients to the molecular level, as well as accepted mechanical properties.

Decoy flares were developed via granulation and subsequent pressing. This approach can ensure good homogeneity and integrity; it includes 5 main stages as follow:

1. Fine powder less than 300 μm with particle size distribution of Al 80 wt% (250-300 μm) and 20 wt% (<250 μm). Teflon white powder with grain size 10 wt%<2 μm, 90 wt%<20 μm.
2. Intimate mixing of oxidizer, fuel, and binder
3. Granulation was performed to retain the homogeneity of the composition. Alternatively, light and dense materials might segregate during transportation, processing, and storage.
4. Filling, by loading 25 g of the composition into metal cylinder of 2.5 cm diameter.
5. The final product was achieved by applying a pressure about 200 atm.

Figure 4 shows the main steps for manufacture of ATV flares.

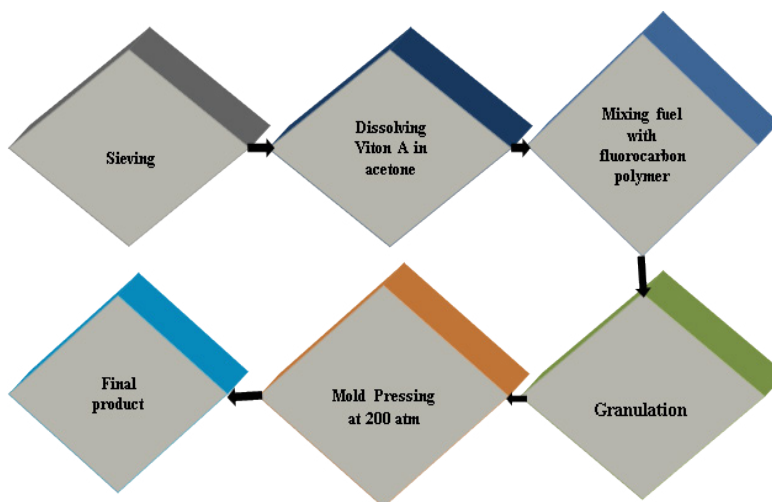


Figure 4: The main manufacture steps of decoy flares.

All investigated compositions were prepared with the same methodology, to avoid any variability, which would affect the performance.

Thermal Signature Measurements

Thermal signature measurement, of developed flares, was conducted using FT-MIR spectrophotometer with spectral range 1-6 μm. The employed setup for spectral measurements includes combustion chamber, optical fibers, spectrophotometer, and data receiving and recording system (**Figure 5**).

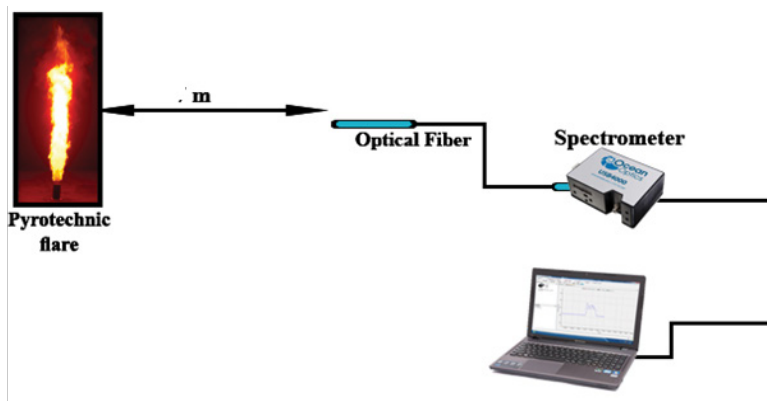


Figure 5: The main manufacture steps of decoy flares.

The inlet of the optical fiber was fixed at distance of 1.5 m from the tested flare. Thermal signature was recorded in counts/s for each wavelength. After acquiring data, the average intensity of α and β bands was evaluated using MATLABR2014 b software.

Results and Discussion

Thermal Signature of Aircraft Engine

Thermal signature of aircraft engine demonstrated two main characteristic peaks over α band (2-3 μm) and β band (3-5 μm). The jet engine thermal signature was correlated to black body emission by the nozzle at 690 °C.

Absorption of the IR emission by air (CO_2 and H_2O) could attenuate the signal over the region 3-4 μm due to CO_2 and H_2O IR absorption [31,32]. This jet engine has θ value of approximately 0.3. Figure 6 demonstrates the thermal signature of jet engine nozzle.

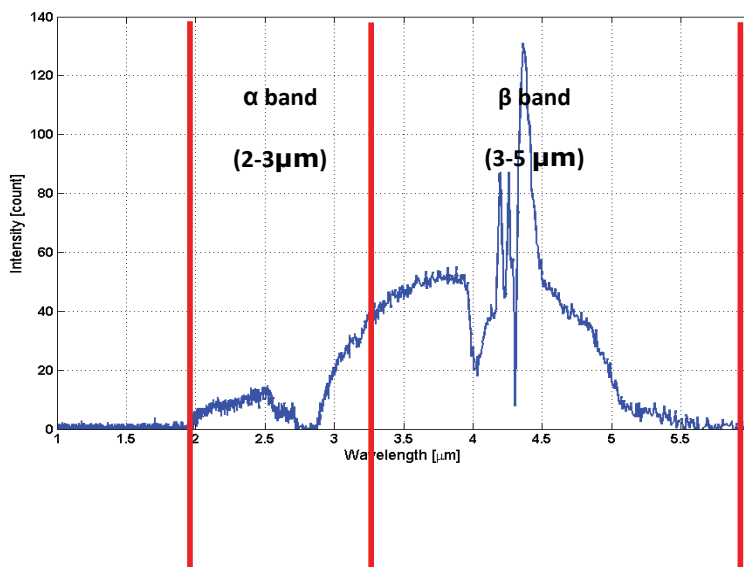


Figure 6: Imprint spectrum of jet engine nozzle.

Thermal Signature of ATV Flares

Thermal signature measurements demonstrated an increase in the intensity of α and β bands with the increase in Al content. Figure 7 demonstrates the IR spectra of the ATV compositions within the band 1-6 μm as function with Al content.

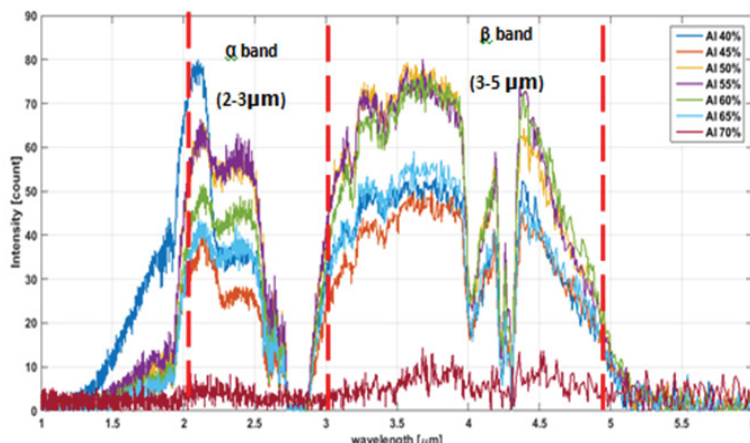


Figure 7: Inprint spectra of ATV flare formulations with different aluminum fuel percentage.

ATV flare with 50 wt% aluminum offered the highest average intensity in the two bands α and β . The average intensity of α and β bands was increased by 6 and 1.5 times, respectively. The relative intensity ratio θ was found to be 0.73. This superior spectral performance can be ascribed to an optimized combustion process, which could maximize the formation of main infrared emitting species (mainly AIF).

It was assumed that aluminum trifluoride (AlF_3) is formed during the reaction of aluminum with teflon [33,34]. The combustion temperature reaches 1275°C ; at this high temperature the formed AlF_3 could be vaporized according to eqn. (7) [30]:



At high temperature AlF_3 could react with metallic Al forming aluminum monofluoride (AIF) (gas) according to eqn. (8) [35,37]:



AIF is the active emitting species in the flame zone. ATV formulation (50% Al) offered the highest percentage (78 wt%) of gas AIF (main IR emitting species), 0.022 wt% Al (metal fuel), and 12.14 wt% carbon soot. Table 3 demonstrates the quantification of combustion products as well as combustion temperature using ICT thermodynamic code.

Table 3: The Impact of fuel percentage on the formation of active emitting species.

Fuel%	C(s)	Al(g)	AIF (g)	AlF_2 (g)	AlF_3 (g)	Al_4C_3 (s)
	wt%	wt%	wt%	wt%	wt%	
40%	14.8	0.088	38.4	30.5	14.7	0
45%	13.6	0.065	58.5	19.3	7.7	0
50%	12.1	0.022	78.1	6.33	2.2	1.055
55%	7.7	0.022	71.04	5.4	1.7	13.99
60%	10.01	25.79(l)	49.2	5.8	9	0
65%	8.5	34.14(l)	42.02	14.9	0	0
70%	7.61	48.067	27.506	4.456	12.267	0

AIF is a molecular species that would emit in the infrared region. This active species could be formed in the primary flame zone (1) next to the burning surface (Figure 8).

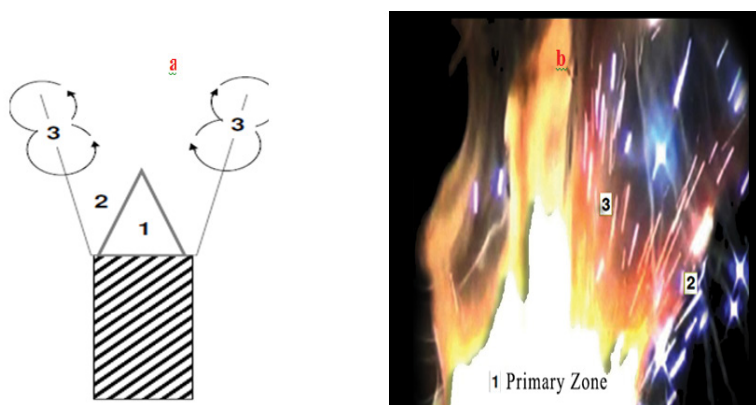


Figure 8: Model for ATV flare combustion (a); practical photo-image for ATV flarecombustion (b).

This primary zone is characterized with high combustion temperature and high density of (carbon soot) heated up by primary combustion products (i.e. AIF). This (carbon soot) at high temperature could be nearly ideal emitter (with $\epsilon=0.9$). Adjacent to the primary reaction zone is a secondary zone (2) (sparks) where Al fuel (small percent in vapor phase) which could be oxidized by air forming Al_2O_3 . The outer zone (3) demonstrates thermally glowing carbonaceous particles that undergo combustion to form CO_2 . Furthermore, formed CO_2 yeild strong peak emission at $2 \mu m$ and strong emission bands at $4.3 \mu m$. At this zone (3) complete oxidation of combustion, products could take place.

Thermal Signature of ATV Flare to Jet Engine Nozzle

Comparative investigation between thermal signature of jet engine nozzle and ATV flare with highest spectral performance was developed. The thermal signature of jet engine was characterized with two characteristic peaks over α and β bands. Average intensity ratio (θ) of the jet engine =0.3. The ATV flare offered similar α and β bands but with higher intensity due to the formation of active IR emitting species in the combustion flame. ATV flare with 50 wt% Al offered an increase in the intensity of α and β bands by 6 and 1.5 times respectively. This formulation offered θ value of 0.73. **Figure 9** demonstrates the thermal signature of jet engine to ATV flare with 50-wt% Al.

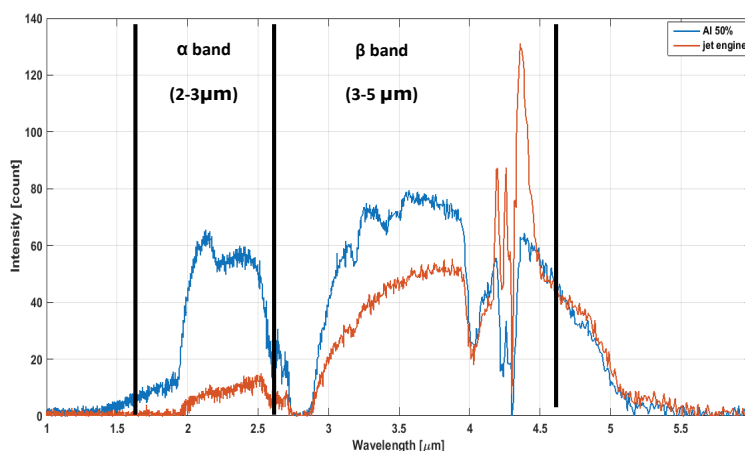


Figure 9: Imprint spectrum of customized Al TV flare to thermal signature of jet engine nozzle.

Effect of Aluminum Content on A and B Bands Average Intensity

The variation of average intensity of α and β bands with aluminum content was evaluated using (mat lab software). **Figure 10** demonstrate the impact of aluminum content on α and β bands average intensity.

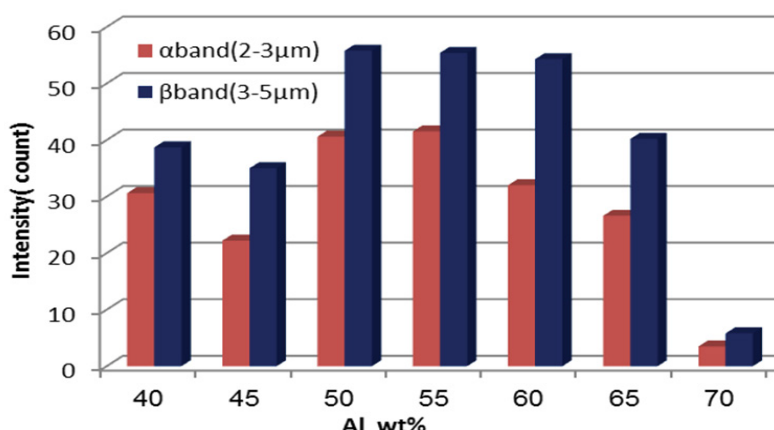


Figure 10: Average intensity of α and β bands as function of Al content.

The effect of Aluminum content can be categorized into three main regions:

- There was unstable burning in α and β bands with Al content (40: 50 wt%)
- The maximum average intensity was at 50% Al percentage.
- There was a decrease in average intensity with Al content from 50% Al till 70% Al.

CONCLUSION

Flares should have a fuel rich system to enhance ignitability and combustion stability. The major combustion products are AlF (transient state), AlF_3 , Al (L), small amount of Al_2O_3 , carbon soot and carbon dioxide. ATV flare with 50 wt% Al offered an increase in the intensity of α and β bands to that of real jet engine nozzle by 6 and 1.5 times respectively. This enhanced spectral performance was ascribed to the high content of AlF (main infrared emitters) in the combustion products. The oxidation of carbon soot to CO_2 would yield strong peak emission at 2 μm and strong emission bands at 4.3 μm . This paper would open the route for development of ATV flares with customized spectral performance as an effective countermeasure of IR seekers.

REFERENCES

1. Koch EC. Review on pyrotechnic aerial infrared decoys. *Propellants Explosives Pyrotechnics*. 2001;26:3-11,.
2. Scheutzw S. Investigations of near and mid infrared pyrotechnics. *Lmu*. 2012.
3. Mahulikar SP, et al. Infrared signature studies of aerospace vehicles. *Progress in Aerospace Sciences*. 2007;43:218-245,.
4. Koch EC. Pyrotechnic countermeasures: II. Advanced aerial infrared countermeasures. *Propell Explos Pyrot*. 2006.
5. Conkling JA and Mocella C. *Chemistry of pyrotechnics: basic principles and theory*: CRC press. 2010.
6. Koch EC, et al. Metal-Fluorocarbon Pyrolants. XIII: High Performance Infrared Decoy Flare Compositions Based on MgB_2 and Mg_2Si and Polytetrafluoroethylene/Viton Propellants, Explosives. *Pyrotechnics*. 2012;37:432-438.
7. Elbasuney S. Novel Colloidal Nanothermite Particles (MnO_2/Al) for Advanced Highly Energetic Systems. *J Inorg Organomet* Volume 2018;28:1793-1800.
8. Elbasuney S, et al. Super-Thermite ($\text{Al}/\text{Fe}_2\text{O}_3$) Fluorocarbon Nanocomposite with Stimulated Infrared Thermal Signature via Extended Primary Combustion Zones for Effective Countermeasures of Infrared Seekers. *J Inorg Organomet P*. 2018.
9. Elbasuney v, et al. Stabilized super-thermite colloids: A new generation of advanced highly energetic materials. *Applied Surface Science*. 2017;419:328-336.
10. Mohamed AK, et al. Nanoscopic fuel-rich thermobaric formulations: Chemical composition optimization and sustained secondary combustion shock wave modulation. *J Hazard Mater*. 2016;301:492-503.
11. Conkling J and Mocella C. Eds *Chemistry of Pyrotechnics Basic Principles and Theory*. London: CRC. 2012.
12. Kosanke KL and Kosanke BJ. Selected Pyrotechnic Publications of KL and BJ Kosanke, Part 1: 1981 Through 1989: *Journal of Pyrotechnics*. 1995.
13. Doty RC, et al. Extremely stable water-soluble Ag nanoparticles. *Chem Mater*. 2005;17:4630-4635.
14. Ritter H and Braun S. High explosives containing ultrafine aluminum ALEX. *Propell Explos Pyrot*. 2001;26:311-314.
15. Yen NH and Wang LY. Reactive metals in explosives. *Propell Explos Pyrot*. 2012;37:143-155.
16. Dreizin EL. Metal-based reactive nanomaterials. *Prog Energ Combust*. 2009;35:141-167.
17. Koch EC. 2006-2008 Annual Review on Aerial Infrared Decoy Flares. *Propell Explos Pyrot*. 2009;34:6-12.
18. Ellern H. *Military and civilian pyrotechnics*. 1968.
19. Koch EC, et al. Combustion behaviour of binary pyrolants based on Mg, MgH_2 , MgB_2 , Mg_3N_2 , Mg_2Si and polytetrafluoroethylene. *Proceedings of the 37th int Pyro Seminar (europyro 2011)*, 2011.
20. Koch EC. Metal-Fluorocarbon-Pyrolants IV: Thermochemical and Combustion Behaviour of Magnesium/Teflon/Viton (MTV). *Propell Explos Pyrot* 2002;27:340-351.
21. Webb R. Searching for Environmentally-Friendly Coloured Fireworks. 4th International Symposium on Fireworks 1998.
22. Fetherolf B, et al. Combustion characteristics and CO_2 laser ignition behaviour of boron/magnesium/PTFE pyrotechnics. 14th International Pyrotechnics Seminar 1989;22.
23. Koch EC. Metal/fluorocarbon pyrolants: V. theoretical evaluation of the combustion performance of metal/fluorocarbon pyrolants based on strained fluorocarbons. *Propell Explos Pyrot* 2004;29:9-18.
24. Koch EC. Theoretical considerations on the performance of various fluorocarbons as oxidizers in pyrolant systems. *International Annual Conference of the Fraunhofer*. 2003.
25. Nielson DB and Lester DM. Extrudable black body decoy flare compositions ed: Google Patents. 2002.
26. Koch EC. Metal-fluorocarbon pyrolants: VIII. Behaviour of burn rate and radiometric performance of two magnesium/Teflon/Viton (MTV) formulations upon addition of graphite. *Journal of Pyrotechnics*. 2008;27:38.
27. Kubota N, Serizawa C. Combustion process of Mg/TF pyrotechnics. *Propell Explos Pyrot*. 1987;12:145-148.

28. Kuwahara T, Ochiai T. Burning rate of Mg/TF pyrolants. *Journal of the Industrial Explosives Society*. 1992;53:301-301.
29. Yarrington C, et al. Combustion Properties of Silicon/Teflon/Viton and Aluminum/Teflon/Viton Composites in 47th AIAA Aerospace Sciences Meeting including The New Horizons Forum and Aerospace Exposition 2009.
30. Yarrington CD, et al. Combustion of silicon/teflon/viton and aluminum/teflon/viton energetic composites. *J Propul Power*. 2010;26:734-743.
31. Yi KJ, et al. Infrared Signature Study of Aircraft Exhaust Plume. in *The 15th International Symposium on Transport Phenomena and Dynamics of Rotating Machinery*. 2014.
32. Guarnieri JA and Cizmas PG. A method for reducing jet engine thermal signature. *International Journal of Turbo and Jet Engines*. 2008;25:1.
33. Yoo S, et al. Modeling kinetics for the reaction of aluminum and teflon and the simulation of its energetic flow motion. *AIP Conference Proceedings* 2012:351-354.
34. Osborne DT. The effects of fuel particle size on the reaction of Al/Teflon mixtures. Texas Tech University. 2006.
35. Witt W and Barrow R. The heat of sublimation of aluminium trifluoride and the heat of formation of aluminium monofluoride. *T Faraday Soc*. 1959;55:730-735.
36. Dyke J et al. A study of aluminium monofluoride and aluminium trifluoride by high-temperature photoelectron spectroscopy. *Chem Phys*. 1984;88:289-298.
37. Conner RW and Dlott DD. Comparing boron and aluminum nanoparticle combustion in Teflon using ultrafast emission spectroscopy. *The Journal of Physical Chemistry*. 2012;116:2751-2760.